Transcriptome and metabolome profiling of field-grown transgenic barley lack induced differences but show cultivar-specific variances

Karl-Heinz Kogel[a], Lars M. Voll[b], Patrick Schäfer[a,c,d], Carin Jansen[a,c,d,1], Yongchun Wu[c,d], Gregor Langen[a], Jafargholi Imani[a], Jörg Hofmann[b], Alfred Schmiedl[b], Sophia Sonnewald[b], Diter von Wettstein[a,c,2], R. James Cook[c,d], and Uwe Sonnewald[b,2]

[a]Research Centre for Biosystems, Land Use, and Nutrition, Justus Liebig University, 35392 Giessen, Germany; [b]Chair Department of Biochemistry, Friedrich-Alexander-University Erlangen-Nuremberg, 91058 Erlangen, Germany; and [c]Department of Crop and Soil Sciences and [d]Department of Plant Pathology, Washington State University, Pullman, WA 99164

Contributed by Diter von Wettstein, February 19, 2010 (sent for review December 9, 2009)

The aim of the present study was to assess possible adverse effects of transgene expression in leaves of field-grown barley relative to the influence of genetic background and the effect of plant interaction with arbuscular mycorrhizal fungi. We conducted transcript profiling, metabolome profiling, and metabolic fingerprinting of wild-type accessions and barley transgenics with seed-specific expression of (1,3-1, 4)-β-glucanase (GluB) in Baronesse (B) as well as of transgenics in Golden Promise (GP) background with ubiquitous expression of codon-optimized *Trichoderma harzianum* endochitinase (ChGP). We found more than 1,600 differential transcripts between varieties GP and B, with defense genes being strongly overrepresented in B, indicating a divergent response to subclinical pathogen challenge in the field. In contrast, no statistically significant differences between ChGP and GP could be detected based on transcriptome or metabolome analysis, although 22 genes and 4 metabolites were differentially abundant when comparing GluB and B, leading to the distinction of these two genotypes in principle component analysis. The coregulation of most of these genes in GluB and GP, as well as simple sequence repeat-marker analysis, suggests that the distinctive alleles in GluB are inherited from GP. Thus, the effect of the two investigated transgenes on the global transcript profile is substantially lower than the effect of a minor number of alleles that differ as a consequence of crop breeding. Exposing roots to the spores of the mycorrhizal *Glomus* sp. had little effect on the leaf transcriptome, but central leaf metabolism was consistently altered in all genotypes.

food safety | glucanase | chitinase | sustainability

Breeding for improved grain weight, higher grain yield, disease resistance, and climatic adaptation by selection of spontaneous mutations shaped the modern barley (*Hordeum vulgare* L.) crop plant beginning as early as 10,000 years ago. With the technical advance to generate transgenic crops with improved agronomic performance, it has become necessary to assess the substantial equivalence of transgenic crop plants; that is, validate that no undesired side effect of the genetic modification has occurred relative to their parental lines (see ref. 1 for review). The availability of the "omics" techniques opens the possibility to probe substantial equivalence in nontargeted global analyses, providing unbiased results.

We have recently developed a 44-K barley microarray based on the assembly of 444,652 barley ESTs into 28,001 contigs and 22,937 singletons, of which 13,265 are represented on the array (2). In contrast, a comprehensive analysis of the metabolome (i.e., all metabolites in a specimen) is not possible because of the immense diversity of primary and secondary plant metabolites (3, 4). Thus, investigating the metabolome requires the prioritization of metabolite subsets as defined by their physicochemical properties or abundance. Although approaches to metabolite profiling are fueled by a multitude of individual targeted metabolite assays of high specificity and accuracy, metabolite fingerprinting aims at obtaining global metabolite patterns by NMR- or MS-based applications, only allowing for suboptimal recovery of individual metabolites (3).

When applied to pathway-engineered transgenic plants, global transcriptome and metabolome analyses could not reveal substantial differences between genetically modified (GM) and non-GM plants. No significant alterations in transcriptome were exhibited in wheat plants expressing *Aspergillus fumigatus* phytase compared with the corresponding non-GM variety, except for changes associated with seed development (5). Similarly, GC-MS-analyzed fructan-producing transgenic potato tubers did not exhibit significant changes, except for metabolites directly connected to the introduced pathway (6), and *Arabidopsis* expressing up to three *Sorghum bicolor* genes involved in the biosynthesis of the cyanogenic glucoside dhurrin did not exhibit any robust transcriptional changes compared to the parental lines (7).

Assessing the influence of natural genotypic variation and environmental factors on multiparallel datasets is of paramount importance to better evaluate the impact of transgene expression. To avoid unnecessary bias, the regarded transgene should not directly influence metabolic pathways in the target plant. An NMR comparison of wheat-flour metabolome derived from field-grown transgenic wheat expressing high molecular weight glutenin and the corresponding parental line revealed that, despite some differences in central free amino acid and sugar metabolism between GM and non-GM varieties, year and field site had a stronger effect on the dataset than expression of the transgene (8). Metabolome analysis of *Bt*-maize by NMR also revealed significant differences in free amino acid contents of the parental line; however, other likely-influential factors were not assessed in this study (9). Comparative transcript profiling of different maize cultivars harboring an identical *Bt* transgene insertion event revealed that the variability between cultivars was much greater than the influence of the transgene (10, 11). Independently, comparison of the potato tuber proteome of 21

Author contributions: K.-H.K., D.v.W., R.J.C. and U.S. designed research; P.S., C.J., Y.W., G. L., J.I., J.H., A.S., and S.S. performed research; K.-H.K., L.M.V., S.S., and U.S. analyzed data; and K.-H.K., L.M.V., and U.S. wrote the paper.

The authors declare no conflict of interest.

Freely available online through the PNAS open access option.

Data deposition footnote: Microarray data obtained in this study can be accessed at http://www.ncbi.nlm.nih.gov/geo/query/acc.cgi?acc=GSE19296.

[1]Present address: Fraunhofer Institute for Molecular Biology and Applied Ecology, Forckenbeckstr. 6, 52074 Aachen, Germany.

[2]To whom correspondence may be addressed. E-mail: diter@wsu.edu or usonne@biologie.uni-erlangen.de.

This article contains supporting information online at www.pnas.org/cgi/content/full/1001945107/DCSupplemental.

tetraploid cultivars with eight potato landraces and five transgenic potato lines led to the same conclusion (12).

In the present study, we investigated two transgenic barley cultivars. The first, hereafter termed ChGP, was designed for ubiquitous expression of a secreted, codon-optimized 42-kDa endochitinase *cThEn(GC)* from *Trichoderma harzianum* (13) in the variety Golden Promise (GP). *Trichoderma* chitinases can degrade rigid fungal cell walls of mature hyphae, conidia, chlamydospores, and sclerotia, in addition to the soft structure of hyphal tips (14–16). Recombinant *cThEn(GC)* conferred growth inhibition to the necrotrophic fungal root pathogens *Rhizoctonia oryzae* and *Rhizoctonia solani* AG8 in vitro (13). Overexpression of *cThEn(GC)* in tobacco and potato yielded high levels of transgene expression, and the transgenics displayed medium-level to complete-resistance phenotypes toward the necrotrophic fungal pathogens *Alternaria alternata*, *Alternaria solani*, *Botrytis cinerea*, and *R. solani* (17).

The second transgenic line employed in the study was pJH271 Beta-Glu-307 (271.06 × Baronesse), hereafter termed GluB, that exhibits hordein-D-promoter-driven, endosperm-specific expression of the chimeric heat-stable (1,3-1,4)-β-glucanase from *Bacillus amyloliquefaciens* and *Bacillus macerans* (18). The GluB transgenics were generated in the GP background, outcrossed to the elite cultivar Baronesse (B), and selected for high yield and good field performance by the single-seed descent method. GluB plants accumulate the recombinant enzyme in storage protein vacuoles and lack β-glucan in endosperm cell walls (19, 18). Expression of (1,3-1,4)-β-glucanase in the endosperm improves the nutritional value of barley for poultry (20, 21).

Making use of comparative, parallel transcriptome profiling, targeted metabolome profiling, and nontargeted metabolite fingerprinting, the present study assesses substantial equivalence in leaves of field-grown transgenic barley relative to the variation between cultivars and to the effects caused by the interaction with mycorrhizal fungi.

Results

Generation and Analysis of Transgenic Barley Plants Expressing Recombinant *Trichoderma* Endochitinase. We constitutively expressed the codon-optimized recombinant *T. harzianum* endochitinase ThEn42(GC) (13) in barley *cv.* Golden Promise either (*i*) fused to the barley chitinase 26 (HvChi26) secretion signal peptide driven by the Cauliflower mosaic virus 35S (CaMV 35S) promoter (Fig. S1*A*) or (*ii*) fused to the chitinase 33 (HvChi33) secretion signal peptide and driven by the maize ubiquitin promoter (Fig. S1*B*). After identification of primary transformants with expression of recombinant endochitinase by immunological detection and subsequent selection for homozygous T_1 transformants (*SI Materials and Methods*), we chose for further study two Ubi::ChGP (Ubi::ChGP-9 and -19) transgenic lines and one 35S::ChGP transgenic line that exhibited the strongest endochitinase expression. We assayed tissue specificity of chitinase activity (Fig. 1*A* and *SI Materials and Methods*, with a quantitative method using the fluorogenic substrate methylumbelliferyl-chitotrioside (Fig. S2*A*). Chitinase activity was highest in coleoptiles, reaching up to 320 $\mu g \cdot g^{-1}$ FW in both Ubi::ChGP lines and 280 $\mu g \cdot g^{-1}$ FW in 35S::ChGP-36 (Fig. 1*A*). Although CaMV 35S-driven chitinase expression in roots was close to that in leaves, ubiquitin-promoter-driven chitinase expression was 6- and 3-fold lower in roots compared with primary leaves or coleoptiles, respectively. Both Ubi::ChGP lines yielded very similar results.

To assess, whether chitinase expression confers antifungal activity, we checked if resistance to *R. solani* AG8 was increased in the transgenics, being quantified as number of wilted leaves per plant (Fig. 1*B* and *SI Materials and Methods*). Compared with the GP wild-type, only 35S::ChGP plants exhibited significantly milder disease symptoms after 1 week of cocultivation with *R. solani* AG8. This finding suggests that, despite the proof of concept obtained from the 35S::ChGP plants, endochitinase amounts might be too low in roots of the two Ubi::ChGP lines to diminish susceptibility toward the highly virulent *R. solani* AG8. Nevertheless, we selected line Ubi::ChGP-9 for further experiments to minimize effects of chitinase expression on the growth of challenging fungi in the field, which could influence both the transcriptome and the metabolome.

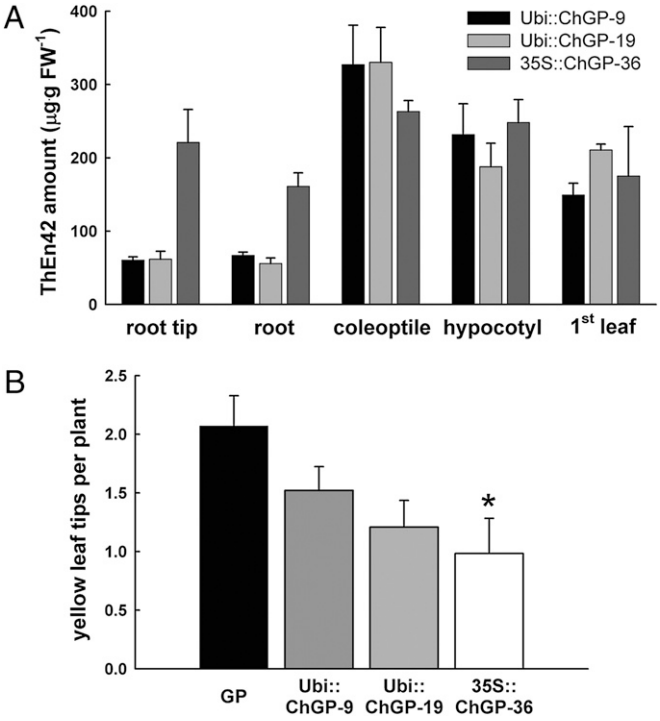

Fig. 1. Characterization of ChGP transformants tissue-specific accumulation of endochitinase ThEn42 in ChGP transformants and its effect on root infections by *R. solani* AG8. (*A*) Amounts of endochitinase in tissues of ChGP transformants. Seedlings of the transgenic barley lines Ubi::ChGP-9 (black bars), Ubi::ChGP-19 (light gray bars), and 35S::ChGP-36 (dark gray bars). Endochitinase content in root tips, upper parts of the roots, coleoptiles, hypocotyls, and first leaves (*Left* to *Right*) were determined with a fluorometric assay (Fig. S2*A* and *SI Materials and Methods*). Data are the mean of five replicate samples ± SEM (*B*) Reduced disease symptoms on ChGP transformants after root inoculation with *R. solani* AG8 (*SI Materials and Methods*). Significant differences to GP with $P < 0.05$ are indicated by an asterisk above the bars and were calculated with a Welch's modified *t* test (29).

Metabolome Analysis of Field-Grown Barley Leaves. We conducted both a targeted metabolite profiling and a metabolite fingerprinting approach with field-grown plants of the four barley genotypes GP, ChGP, B, and GluB that were cultivated in the field at the Giessen Experimental Station (Giessen, Germany; *SI Materials and Methods*). The plants were grown with and without amendment of soil in the plots with Amykor (Amykor Wurzel-Vital), a mixture of the mycorrhizal fungi *Glomus mosseae* and *Glomus intraradices*. Targeted analysis of 72 metabolites, including major carbohydrates, free amino acids, carboxylates, phosphorylated intermediates, major antioxidants (such as ascorbate, glutathione, and tocopherol), as well as carotenoids (for complete dataset, see Table S1), revealed only three differences associated with endochitinase expression in the GP background. In contrast, the contents of sucrose, starch, the amino acids Gln, Ala, and Leu, as well as of the carboxylate oxoglutarate were significantly reduced in GluB compared to B (Table S1). Comparisons of the two unmodified varieties B and GP revealed more consistent differences (e.g., UDPGlc and the amino acids, Tyr, Phe, Ala, Leu, and Cys) (Fig. 2*A*). Furthermore, several consistent changes in central leaf metabolism

in response to Amykor treatment were revealed (Fig. 2*B*): although the amounts of free hexoses and central phosphorylated intermediates (3PGA, PEP, RuBP, Glc1P), free inorganic phosphate and the carboxylates isocitrate and malate increased upon treatment, the contents of sucrose, the two major amino acids Glu and Asp, as well as chlorophyll, lutein, and glutathione all decreased in response to mycorrhizal inoculation (Fig. 2*B*).

The elevated pool sizes of several phosphorylated intermediates indicate improved phosphate availability as a possible consequence of successful mycorrhizal root colonization. Thus, it was instructive to determine the extent of mycorrhizal root colonization in plots with and without treatment with Amykor. Quantification of fungal genomic DNA by qPCR based on the *G. mossae* ITS sequence relative to host ubiquitin revealed increased fungal abundance in roots from treated compared with untreated plots (Fig. S3), despite considerable amounts of fungal DNA in plants (e.g., in GP) from untreated plots. Furthermore, microscopic analysis of plants grown in plots treated with Amykor confirmed arbuscle formation in all specimens (*SI Materials and Methods*), demonstrating that mycorrhiza were intact and functional. To validate that the characteristic changes in the leaf metabolome were brought about by improved mycorrhizal colonization of plants in the Amykor-treated plots, we determined the same targeted metabolome profile of ChGP and GP plants grown under controlled conditions in the greenhouse with soil that was either devoid of mycorrhizal inoculum or fortified with the same dosage of Amykor as in the field experiment. The contents of phosphorylated intermediates and hexoses were altered in a similar fashion between mycorrhizal and non-mycorrhizal plants of both examined genotypes in the field and in the greenhouse experiment (Table S2), providing strong indication for successful symbiotic interactions in all genotypes in the field experiment (*SI Materials and Methods*).

In a principal component analysis (PCA), the targeted metabolome data were able to distinguish both the effect of mycorrhizal infection and cultivar-specific differences by principal components 1 (PC1) and PC2, respectively (Fig. 3*A*; see Fig. S4*A* for the corresponding hierarchical cluster analysis). Interestingly, the metabolite profile in GluB transgenics was less affected by mycorrhizal infections compared to the other genotypes, and GluB was more distant to non-GM B plants than the ChGP transgenics was from their wild-type counterpart. As indicated by individual metabolite contents (mentioned in the previous paragraph), sugars, major amino acids, and phosphorylated intermediates strongly loaded on PC1 in response to mycorrhizal infections. Likewise, sugar and free amino acid contents contributed strongly to PC2, distinguishing cultivar-specific differences. Nearly identical results were obtained when data from the 307 most significant mass signals of a metabolite fingerprinting approach were fed into the PC analysis (Fig. 3*B*), except that GP and ChGP were more distant to each other in the Amykor treatment compared to untreated samples.

Transcriptome Analysis of Field-Grown Barley Leaves. Our next goal was to compare the discriminatory power of the metabolome analysis to that of the corresponding transcriptome dataset obtained from identical sample pools (*SI Materials and Methods*). PCA resulted in a similar discrimination of genotypes as reported for the metabolome analyses, with GluB again being distant from B (Fig. 3*C*; see Fig. S4*B* for the corresponding hierarchical cluster analysis). In contrast to the metabolome analysis, treatment with Amykor could not be clearly resolved in the PC analysis; indeed, no statistically significant differentially transcribed genes were detected in three of the four examined genotypes in response to the Amykor treatment. Only in GP, 4 out of 31,198 features detected on the array were differentially expressed in response to the mycorrhizal fungi (Table S3). However, 1,660 genes (697 up

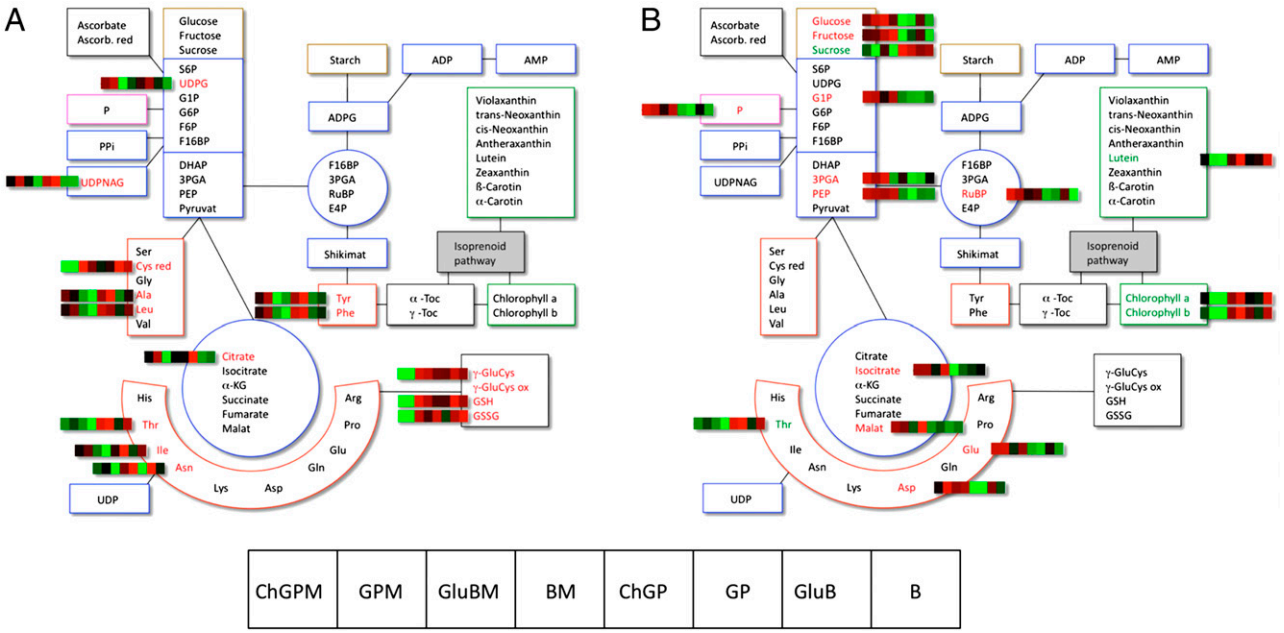

Fig. 2. Differentially abundant metabolites in barley leaves. Overview of differentially abundant metabolites from the targeted profiling approach with leaf material from 4-month-old, field-grown barley plants representing the treatments (*A*) cultivar or (*B*) Amykor. The schematic metabolic diagrams in (*A*) and (*B*) represent a map of all analyzed metabolites. The heat map strips next to the metabolite names were taken from the hierarchical cluster analysis (Fig. S4*A*) conducted with the program Cluster v2.11 (30), with red signals denoting an increased metabolite content relative to average and green signals indicating decreased metabolite contents relative to average. The consistent sample order in these strips is indicated at the bottom of the figure using the genotype and treatment abbreviations used throughout the text and as explained below. The entire dataset, including the results of the significance tests, are given in Table S1. Please note that the color pattern has no implications on statistically significant differences in pairwise comparisons, which were calculated with a Welch-Satterthwaite test embedded in the VANTED software v1.7 (31) and are displayed in Table S1. GP, Golden Promise; B, Baronesse; ChGP, Chitinase GP; GluB, Glucanase B; M, Amykor treatment.

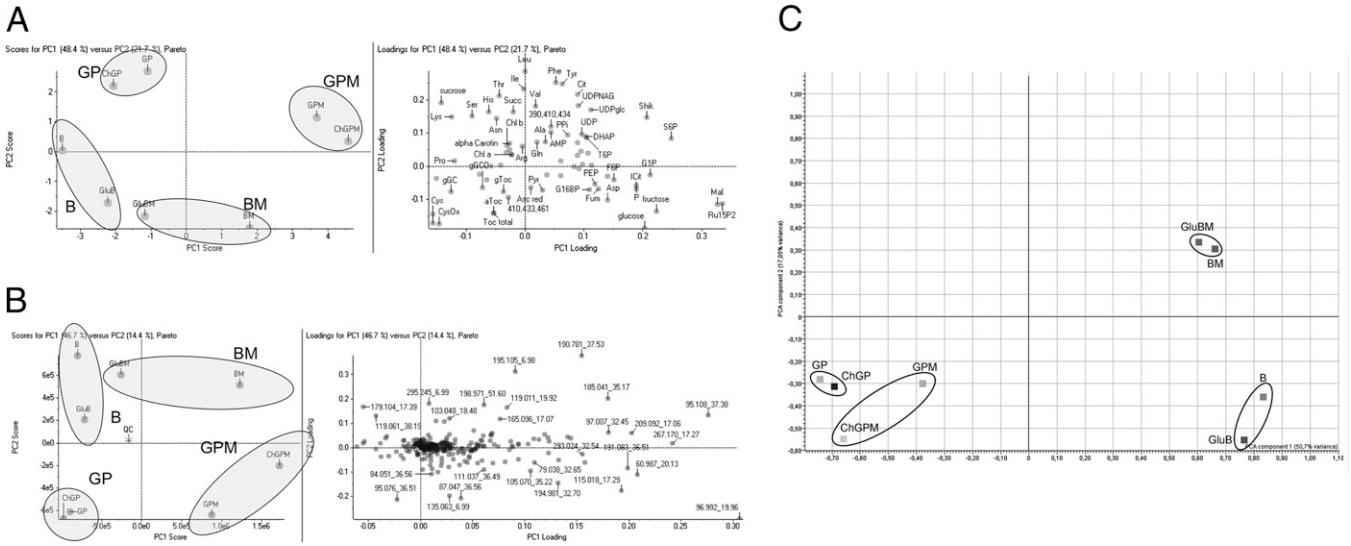

Fig. 3. Principal component analysis (PCA) of multiparallel datasets obtained from field-grown barley leaves. (*A*) PCA based on 72 metabolites that were analyzed in a targeted fashion (complete dataset displayed in Table S1): For PCA, mean values of four replicate samples per genotype and treatment were taken and the resulting data points labeled as described below. (*Left*) PCA plot of principal component 1 (PC1) versus principal component 2 (PC2). Circles are drawn around spots derived from the genotype of identical cultivar or treatment and are labeled by letters as indicated below. (*Right*) loadings plot for PC1 and PC2. The 72 metabolites are individually labeled. (*B*) PCA of metabolite fingerprinting data. The analysis was computed for the 307 most significant mass signals obtained by metabolite fingerprinting and is based on mean values from four replicate samples (see *Materials and Methods*). Compounds are labeled according to the quantified transition. Data arrangement and labeling are as described in *A*. (*C*) PCA of transcriptome data. PCA was performed based on data from two replicate hybridizations per genotype and treatment. RNA was extracted from aliquots of pooled sample material also used for metabolome analysis. From the 1,660 genes differentially expressed between cultivars B and GP (Table S3), five of the most significant ones were confirmed by qRT-PCR analysis of independent sample aliquots (Fig. S2*B*). GP, Golden Promise; B, Baronesse; ChGP, Chitinase GP; GluB, Glucanase B; M, Amykor treatment.

and 863 down) were differentially transcribed between the cultivars GP and B (Tables S3 and Dataset S1), indicating strong cultivar-specific expression patterns. The result of the microarray data analysis was confirmed in independent sample pools by qRT-PCR, picking five genes with cultivar-specific transcript abundance (Fig. S2*B*). Along with genes involved in carbohydrate metabolism and genes coding for storage proteins, defense-associated genes were strongly overrepresented among the differentially regulated genes in the GP to B comparison (Fig. S2*C*). This result likely reflects a greater level of disease resistance obtained deliberately or fortuitously over years of breeding and selection for ever better-adapted and higher-yielding modern barley varieties. Of particular interest, 22 differentially transcribed genes were found between GluB and its non-GM counterpart B (Table S3), corresponding with the distance of these two genotypes in the PCA. Sixteen of these 22 differential genes, (i.e., approx. 73%) were also discriminated in the GP to B comparison. Although surprising at first glance, this finding can be explained by the pedigree of GluB. GluB was produced by transformation of GP with glucanase transgene, which was later introduced into the cultivar B by outcrossing and selection of single-seed descendants. Thus, differential gene expression between GluB and B could be caused by retention of a few GP alleles in the GluB genotype.

To obtain data in support of this hypothesis, we attempted to refine the chromosomal location of the 16 genes that were differentially transcribed in both the GluB to B and the GP to B comparisons on the current genetic map of barley (http://www.harvest-web.org/hweb/bin/gmap.wc?wsize=1263 × 854). Although 14 of the unigenes had no assigned map position, 2 could be located between 142 cM and 167 cM on the lower arm of chromosome 7H. Analysis of two simple sequence repeat (SSR) markers located in the region of interest revealed that both carried the GP allele (Fig. 4 and Fig. S5).

Discussion

The comprehensive dataset generated in the present study provides a comparison of the alterations in leaf transcriptome and metabolome caused by (*i*) the presence of transgenes, (*ii*) cultivar, and (*iii*) biotic interactions in the root. This dataset leads us to four major conclusions.

First, the effect of recombinant *Trichoderma* chitinase on both the metabolome and transcriptome was negligible compared to the differences between the wild-type cultivars GP and B.

Second, the metabolome analysis has proven to be as sensitive as the survey of the corresponding transcriptome as a means to detect minor differences between B and the out-bred transgenic GluB. In addition, both targeted and untargeted metabolome analyses discerned an influence of mycorrhizal infection on leaf

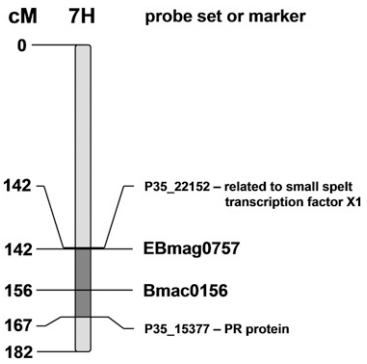

Fig. 4. Inheritance of GP alleles in GluB on the lower arm of barley chromosome 7H. Two of the 16 unigenes differentially expressed in both the B vs. GP and the B vs. GluB comparisons could be mapped to the current physical barley map (www.harvest-web.org) and were located at 142 cM and 167 cM on chromosome 7H, respectively. Analysis of the two polymorphic SSR markers EBmag0757 (142 cM) and Bmac0156 (156 cM) revealed retention of the respective GP alleles in GluB that had been generated by introgressing the *GluB* transgene from GP into B. Locations of the employed markers and the two unigenes of interest on the genetic map are given on the left, their names and annotations are to the right to the chromosomal sketch.

metabolism that was not achieved by transcriptome analysis alone. In targeted experiments, on the other hand, differential display was used successfully to identify transcripts of five differentially expressed genes from leaves of mycorrhiza-colonized tomato (22). Based on our results, metabolome analysis represents a more immediate probe of physiological status of the plant than the transcriptome. We have found that a subset of phosphorylated intermediates of central metabolism was more abundant in leaves of Amykor-treated than in control plants, reflecting improved phosphate availability in treated plants.

Third, comparisons of the metabolome and transcriptome between the transgenic GluB and wild-type B revealed four differentially abundant metabolites and 22 deregulated transcripts, suggesting a more distant positioning in the PCA between these two lines, as compared to ChGP and GP. Although the reason for the deviation in the metabolome of GluB and B remain elusive, about 73% of the differentially transcribed genes between GluB and B were similarly deregulated between GP and B. The evidence for genetic linkage of 2 out of the 16 coregulated genes between GluB and GP by SSR marker analysis indicates that the differences in the transcript profiles of GluB and B could be attributed to retention of introgressed GP traits in the GluB background. This finding could also hold true for the differences in the GluB and B metabolome profiles. Our finding suggests that introgression of a few alleles can convey a stronger effect on substantial equivalence than the introduction of the two regarded transgenes.

Fourth, compared with the previously addressed slight changes, the data compiled for GP and B revealed 1,660 differentially regulated genes and a considerable, albeit minor, number of steady-state metabolite pools that were substantially different. Targeted qRT-PCR analysis of five genes that strongly differed in expression between GP and B disclosed that, for most of them, transcripts were only specifically abundant in one of the two cultivars. Defense-associated genes such as pathogenesis-related gene-4 (*PR-4*) were overrepresented in the 1,660 genes. Because we did not include a substantial number of defense-related metabolites in our targeted metabolome analysis, the difference in defense priming between GP and B remained obscure in the metabolite dataset. As no symptoms of infection were visible on any genotype at sampling date, our data indicates that subclinical or latent infections at the field site had triggered defense-gene expression. Thus, our results suggest that B, unlike GP, was in an alert state with basal expression of pathogenesis-related genes. The variety GP lacks most resistance genes (23) and exhibits a much weaker defense response compared to bred high-end varieties. We can thus estimate that past breeding of elite lines, such as B for putative disease resistance, represent the strongest effect on global gene expression between cultivars in the field, where plants are subjected to perpetual challenge by microbial pathogens and pests. Such large differences are not expected to be caused by single transgenes, although evidence on pathogen-challenged disease-resistant GM crops is thus far unavailable. Although resistance toward pathogen challenge in the field should be increased in ChGP because of the presence of endochitinase, transcript profiles of ChGP, and because GP did not exhibit significant differences, unlike the B to GP comparison described above. This result means that endochitinase expression did not affect the transcriptome in challenged plants. In comparison, strong differences in transcript profiles of Bt maize compared with non-GM cultivars were to be expected upon corn borer infestation, representing sick and healthy plants, respectively.

Conclusion

In summary, our results substantially extend observations that cultivar-specific differences in transcriptome and metabolome greatly exceed effects caused by transgene expression. Furthermore, we provide evidence that, (*i*) the impact of a low number of alleles on the global transcript and metabolite profile is stronger than transgene expression and that, more specifically, (*ii*) breeding for better adaptation and higher yields has coordinately selected for improved resistance to background levels of root and leaf diseases, and this selection appears to have an extensive effect on substantial equivalence in the field during latent pathogen challenge.

Materials and Methods

Barley Seed. The seed used in this study represented barley lines pYW210-9-(4001-4360), pYW210-19-(4701-6100), pYW300-36-(7121-7187), pJH271-Beta Glu-307 and the cultivars Golden Promise and Baronesse. Line pYW210-9-(4001-4360), termed ChGP, and lines pYW210-19-(4701-6100) and pYW300-36-(7121-7187), which are constitutively expressing endochitinase ThEn42 (GC) from *T. harzianum* (13), were produced for this study (see below). Line pJH271-Beta Glu-307, termed GluB, constitutively expresses a thermostable (1,3-1,4)-β-glucanase and was described earlier (18).

Double-Cassette Vector Construction with the Ubiquitin Promoter and Barley Transformation. For construction of plasmid pYW300 (Fig. S1*A*), the Cauliflower mosaic virus 35S promoter was amplified from plasmid *pBI221* (Clontech Inc.), digested with *Hin*dIII and *Pst*I, and inserted into *Hin*dIII- and *Pst*I-digested plasmid pAM110-cTHEn42(GC) (Fig. S1*C*). The *Hin*dIII-*Not*I fragment of this plasmid was moved into pAM300b (Fig. S1*D*), and the *Hin*dIII-*Eco*RI fragment from this intermediate vector was then inserted into the pJH 260 binary vector as described for the vectors with the ubiquitin promoter (see below). The sequence of the plasmid pYW300 has been assigned GenBank Accession number DQ469639.

Plasmid pYW210 (Fig. S1*B*) was constructed in the binary cloning vector pJH260 derived from pBIN19, as follows: The fragment containing *cThEn42(GC)* provided with the *pUbi 1* promoter and the *SP(HvChi33)* signal sequence was excised from plasmid pAM110-cThEn42(GC) (Fig. S1*C*) with *Hin*dIII and *Not*I. The resulting fragment was inserted into *Hin*dIII-/*Not*I-digested plasmid pAM300b (Fig. S1*D*), yielding plasmid pAM300. A *Hin*dIII / *Eco*RI fragment of the insert was cloned into pJH260 to produce plasmid pYW210 (GenBank Accession Number DQ469636). For barley transformation, see *SI Materials and Methods*.

Metabolome Profiling and Metabolite Fingerprinting. Targeted analysis of free amino acids (24), major leaf carbohydrates (25), ascorbic acid, tocopherols and glutathione (26), carotenoids (2), phosphorylated intermediates and carboxylates (27) was conducted as previously described.

Untargeted metabolome profiling by ESI-MS was carried out on a QTrap3200 mass spectrometer (Applied Biosystems) after metabolite extraction and ion exchange chromatography as described (26). Negative Ions were generated at −4.5 kV and a declustering potential of −20 V. The entrance potential was from −6 to −4 V, and gas pressures were 20 psi (curtain), 30 psi (nebulizer), and 20 psi (turbogas). A mass range of *m/z* 60–610 was recorded with one scan per second over 80 min. Peak alignment was performed after import into Marker View (Applied Biosystems) with a retention time tolerance of 0.75 min and a mass tolerance of 1.0 amu. Maximal number of peaks was set to 500. Retention time corrections and normalization was done with the internal standard pipes (*m/z* 301.1; RT 16.6 min). For PC analysis of fingerprinting data, quality control samples were generated as described (28) by pooling equal-volume amounts from all analyzed samples. Artifact peaks were removed before the analysis was conducted with MarkerView.

ACKNOWLEDGMENTS. We thank Christel Nickel-Demuth, Volker Weisel, Udo Schnepp, and Helmut Schepp for assistance with field work. The authors also gratefully acknowledge excellent technical assistance by Stefanie Wisshak and Stephen Reid in quantitative transcript analyses as well as Isabella Zagorski for technical assistance in metabolite analysis. This project was funded by the Bundesministerium für Bildung und Forschung (K.-H.K. and U.S.). The Deutsche Forschungsgemeinschaft granted a Mercator professorship to D.v.W.

1. Cellini F, et al. (2004) Unintended effects and their detection in genetically modified crops. *Food Chem Toxicol* 42:1089–1125.
2. Schäfer P, et al. (2009) Manipulation of plant innate immunity and gibberellin as factor of compatibility in the mutualistic association of barley roots with *Piriformospora indica*. *Plant J* 59:461–474.
3. Fiehn O (2001) Combining genomics, metabolome analysis, and biochemical modeling to understand metabolic networks. *Comp Funct Genomics* 2:155–168.
4. Trethewey RN (2004) Metabolite profiling as an aid to metabolic engineering in plants. *Curr Opin Plant Biol* 7:196–201.

5. Gregersen PL, Brinch-Pedersen H, Holm PB (2005) A microarray-based comparative analysis of gene expression profiles during grain development in transgenic and wild type wheat. *Transgenic Res* 14:887–905.
6. Catchpole GS, et al. (2005) Hierarchical metabolomics demonstrates substantial compositional similarity between genetically modified and conventional potato crops. *Proc Natl Acad Sci USA* 102:14458–14462.
7. Kristensen C, et al. (2005) Metabolic engineering of dhurrin in transgenic Arabidopsis plants with marginal inadvertent effects on the metabolome and transcriptome. *Proc Natl Acad Sci USA* 102:1779–1784.
8. Baker JM, et al. (2006) A metabolomic study of substantial equivalence of field-grown genetically modified wheat. *Plant Biotechnol J* 4:381–392.
9. Manetti C, et al. (2006) A metabolomic study of transgenic maize (*Zea mays*) seeds revealed variations in osmolytes and branched amino acids. *J Exp Bot* 57:2613–2625.
10. Coll A, et al. (2008) Lack of repeatable differential expression patterns between MON810 and comparable commercial varieties of maize. *Plant Mol Biol* 68:105–117.
11. Coll A, et al. (2009) Gene expression profiles of MON810 and comparable non-GM maize varieties cultured in the field are more similar than are those of conventional lines. *Transgenic Res* 18:801–808.
12. Lehesranta SJ, et al. (2005) Comparison of tuber proteomes of potato varieties, landraces, and genetically modified lines. *Plant Physiol* 138:1690–1699.
13. Wu YC, von Wettstein D, Kannangara CG, Nirmala J, Cook RJ (2006) Growth inhibition of the cereal root pathogens *Rhizoctonia solani* AG8, *R. oryzae* and *Gaeumannomyces graminis* var. *tritici* by a recombinant endochitinase from *Trichoderma harzianum*. *Biocontrol Sci Technol* 16:631–646.
14. Cherif M, Benhamou N (1990) Cytochemical aspects of chitin breakdown during the parasitic action of a *Trichoderma* sp. on *Fusarium oxysporum* f. sp. *radicis-lycopersici*. *Phytopathology* 80:1406–1414.
15. Lorito M, et al. (1993) Chitinolytic enzymes produced by *Trichoderma harzianum*: Antifungal activity of purified endochitinase and chitobiosidase. *Phytopathology* 83: 302–307.
16. Lorito M, et al. (1996) Mycoparasitic interaction relieves binding of the Cre1 carbon catabolite repressor protein to promoter sequences of the ech42 (endochitinase-encoding) gene in *Trichoderma harzianum*. *Proc Natl Acad Sci USA* 93:14868–14872.
17. Lorito M, et al. (1998) Genes from mycoparasitic fungi as a source for improving plant resistance to fungal pathogens. *Proc Natl Acad Sci USA* 95:7860–7865.
18. von Wettstein D (2007) From analysis of mutants to genetic engineering. *Annu Rev Plant Biol* 58:1–19.
19. Horvath H, et al. (2000) The production of recombinant proteins in transgenic barley grains. *Proc Natl Acad Sci USA* 97:1914–1919.
20. von Wettstein D, Mikhaylenko G, Froseth JA, Kannangara CG (2000) Improved barley broiler feed with transgenic malt containing heat-stable (1,3-1,4)-β-glucanase. *Proc Natl Acad Sci USA* 97:13512–13517.
21. von Wettstein D, Warner J, Kannangara CG (2003) Supplements of transgenic malt or grain containing (1,3-1,4)-β-glucanase to barley-based broiler diets lift their nutritive value to that of maize. *Br Poult Sci* 44:438–449.
22. Taylor J, Harrier LA (2003) Expression studies of plant genes differentially expressed in leaf and root tissues of tomato colonised by the arbuscular mycorrhizal fungus *Glomus mosseae*. *Plant Mol Biol* 51:619–629.
23. O'Hara RB, Brown JKM (1997) Spatial aggregation of pathotypes of barley powdery mildew. *Plant Pathol* 46:969–977.
24. van Wandelen C, Cohen SA (1997) Using quarternary high-performance liquid chromatography eluent systems for separating 6-aminoquinolyl-N-hydroxysuccinimidyl carbamate derivatized amino acid mixtures. *J Chromatogr A* 763:11–22.
25. Voll L, et al. (2003) The phenotype of the *Arabidopsis cue1* mutant is not simply caused by a general restriction of the shikimate pathway. *Plant J* 36:301–317.
26. Abbasi AR, et al. (2009) Tocopherol deficiency in transgenic tobacco plants leads to accelerated senescence. *Plant Cell Environ* 32:144–157.
27. Horst RJ, et al. (2010) *Ustilago maydis* infection strongly alters organic nitrogen allocation in maize and stimulates productivity of systemic source leaves. *Plant Physiol* 152:293–308.
28. Bijlsma S, et al. (2006) Large-scale human metabolomics studies: a strategy for data (pre-) processing and validation. *Anal Chem* 78:567–574.
29. Welch BL (1947) The generalization of student's problem when several different population variances are involved. *Biometrika* 34:28–35.
30. Eisen MB, Spellman PT, Brown PO, Botstein D (1998) Cluster analysis and display of genome-wide expression patterns. *Proc Natl Acad Sci USA* 95:14863–14868.
31. Junker BH, Klukas C, Schreiber F (2006) VANTED: A system for advanced data analysis and visualization in the context of biological networks. *BMC Bioinformatics* 7:109.